Advances in Colloid and Interface Science xxx (2014) xxx–xxx

Contents lists available at ScienceDirect

Advances in Colloid and Interface Science

journal homepage: www.elsevier.com/locate/cis

On the identification of liquid surface properties using liquid bridges

M. Kostoglou, T.D. Karapantsios *

Department of Chemical Technology, School of Chemistry, Aristotle University, Univ. Box 116, 541 24 Thessaloniki, Greece

ARTICLE INFO

Available online xxxx

Keywords:
Liquid bridge
Surface tension
Thin film
Surfactants
Marangoni convection
Gibbs elasticity

ABSTRACT

The term liquid bridge refers to the specific silhouette of a liquid volume when it is placed between two solid surfaces. Liquid bridges have been studied extensively both theoretically and experimentally during the last century due to their significance in many technological applications. It is worth noticing that even today new technological applications based on liquid bridges continue to appear. A liquid bridge has a well-defined surface configuration dictated by a rigid theoretical foundation so the potential of its utilization as a tool to study surface properties of liquids is apparent. However, it is very scarce in literature that the use of liquid bridges is suggested as an alternative to the well-established drop techniques (pendant/sessile drop). The present work (i) presents the theoretical background for setting up a liquid-bridge based surface property estimation problem, (ii) describes the required experimental equipment and procedures and (iii) performs a thorough literature review on the subject. A case with particular interest is that of liquid bridges made of electrically conducting liquids forming between two conducting solids; such a liquid bridge presents an integral electrical conductance value which is sensitive to the specific silhouette of the bridge. This enables the use of this integral conductance as shape descriptor instead of the conventional image processing techniques. Several attempts in literature for the estimation of liquid surface tension, liquid–solid contact angle and surfactant induced surface elasticity for conducting or non/conducting liquids are presented and the prospects of the technique are discussed.
© 2014 Elsevier B.V. All rights reserved.

Contents

1. Introduction

Small liquid amounts connecting two solid surfaces, apart by a short distance, are defined as liquid bridges. These solid surfaces can be surrounded by a gas phase or can be immersed in another liquid immiscible to that of the liquid bridge. The present work refers mainly to the first case which is the most common. The theoretical and experimental study of these liquid formations has been very extensive during the last century. The shape of liquid bridges of pure liquids is determined by intermolecular forces (liquid to liquid molecular interaction determines surface tension whereas the three phase contact line is additionally influenced by liquid to solid molecular forces), by gravity and by external fields such as an electrostatic one. Although liquid bridges refer to small liquid volumes, they can be found in a range of size scales. Regarding the upper size scale there is a limit at the physical dimension of about 1 cm. At this size, gravity causes spontaneous collapse of liquid bridges. Even in the absence of gravity (space station experiments or by density matching with the surrounding fluid) there is the so-called Rayleigh stability limit at which some oscillation modes of the bridge

* Corresponding author.
E-mail address: karapant@chem.auth.gr (T.D. Karapantsios).

http://dx.doi.org/10.1016/j.cis.2014.04.007
0001-8686/© 2014 Elsevier B.V. All rights reserved.

Please cite this article as: Kostoglou M, Karapantsios TD, On the identification of liquid surface properties using liquid bridges, Adv Colloid Interface Sci (2014), http://dx.doi.org/10.1016/j.cis.2014.04.007

ARTICLE IN PRESS

become unstable leading to its disintegration to droplets. For bridges smaller than about 1 mm the effect of gravity is negligible and intermolecular forces completely dominate their shape. There is no lower limit to the bridge physical size beyond that imposed by the molecular nature of the liquid. The situation in the presence of surfactants is much more complex. These molecules not only affect the equilibrium surface tension of the liquid but also bring about a dynamic interfacial behavior of the bridge as they diffuse slowly from the bulk of the bridge towards the gas–liquid interface.

There are many technological applications where liquid bridges are encountered. A non-exhaustive list includes processes such as granulation, flotation and coating [1–3]. In mechanical engineering, liquid bridges allow control of forces in micro-gripping processes [4]. In geology, liquid bridges determine the properties of moist soil. They are also related to the tertiary oil recovery from porous media. A particular recent area of interest refers to self assembly of particles for which surface tension is the main driving force [5]. New technologies for fabrication of micro-electromechanical systems based on liquid bridges have been proposed [6]. Liquid bridges have been employed as dispensing devices in medical applications [7]. Liquid bridges formed between the tip of the atomic force microscopy probe and the analyzed sample (in humid environment) affects significantly the measurements [8,9]. Despite the plethora of experimental and theoretical studies on liquid bridges it is surprising that very few refer to the presence of surfactant in the liquid bridge [10,11]. On the contrary, many works deal with the stability of the bridge with respect to stretching [12], air shearing [13] or thermocapillary effect [14]. The attempts of using liquid bridges as diagnostic tools to estimate liquid or surfactant properties are very limited. As a matter of fact, only one work apart from those examined in detail below was found to refer to a qualitative assessment of the rheological properties of biological fluids [15].

Here some ideas are presented on using liquid bridges as vehicles to measure surface properties of liquids and the up to now progress is reported. It is well established that the shape of a liquid bridge depends on surface properties. So the main idea lies at the possibility to deduce surface properties by tracing this shape. The straightforward way would be to employ optical images of a liquid bridge and to process it appropriately through the solution of the Young–Laplace equation. This technique is similar to the respective technique developed for pendant drops [16,17]. However, optical imaging is hampered by inevitable ambient vibrations which blur the bridge shape lowering the accuracy of determinations. Proper illumination conditions yielding high contrast at the bridge borders, high resolution of optical and digital devices and slow image recording/processing steps are further drawbacks of this approach. A different (integral) technique is based on the measurement of forces produced by liquid bridges between the two supporting solid surfaces. This type of measurement suffers excessively from ambient vibrations which cause stability problems and add high background noise to force measurements lowering the accuracy and requiring extensive data filtering [18]. Another integral technique measuring a property indicative of the shape of a bridge is based on the liquid bridge's electrical conductance. This is a much simpler technique than optical imaging or force measurement and calls for passing low intensity alternating electrical current through the bridge and measuring current intensity and voltage. This technique must be not confused with the extensively studied application of electrical fields to create/stabilize liquid bridges of dielectric or slightly conducting liquids [19,20] or soap films of conducting liquids [21].

The proposed electrical technique cannot be applied to a pendant or sessile drop without interfering with the drop shape. In the case of a liquid bridge, the technique is applied naturally as long as the employed liquid is electrically conductive and the bridge solid supports are from conductive material. Apparently, the possibility of deriving surface properties based on a fast, integral, non-interfering technique needs to be exploited. Several ideas have emerged on this context. The first idea refers to the identification of surface tension. The shape of a liquid bridge is the result of the competition between gravity and surface tension. The conductance of a bridge depends on its shape and, accordingly, on surface tension. The second idea refers to the identification of contact angle. For small liquid bridges of insignificant Bond number the shape of the bridge is fully determined from the contact angle with its supports. In this case the conductance is directly related to the contact angle. The third idea refers to the creation of a thin liquid film between the surrounding gas and a bubble produced inside the bridge and to examine its conductance in order to identify surface elasticity, e.g., induced by a surfactant in the liquid.

The structure of the present work is the following: At first the theoretical foundation behind the examined experimental techniques is discussed. Assumptions, simplifications and solution techniques are presented in detail. Then the experimental setup and the corresponding strategies are described. Finally, up to now findings of applying the theory to experimental data are presented and the strategy for the future is discussed.

2. Theoretical framework

2.1. The general problem

Let us consider the most general case considered in the present work, that of a liquid bridge in the presence of a surfactant with the possibility of producing a bubble internally to the bridge. Three types of experiments have been realized differing by the way motion is imposed externally to the system. These types of experiments are: (i) increasing the distance between the solid rods supporting the bridge, (ii) reducing the volume of the bridge by liquid evaporation or by withdrawing of liquid through a hollow supporting rod and (iii) growing the internal bubble by feeding gas through a hollow supporting rod. The direct approach to model the motion of the liquid bridge system is complicated due to the involvement of phenomena occurring simultaneously at different size and time scales. To be more specific the Navier–Stokes equations must be solved for the liquid and the gas in the internal bubble combined to the surfactant mass conservation equation in the liquid phase. The boundary condition for the Navier–Stokes equations includes the continuity of the normal and tangential stresses at the gas–liquid interfaces [22]. The boundary conditions for the surfactant conservation equation includes surfactant adsorption–desorption and its surface diffusion on the gas–liquid interfaces. Interfacial surfactant non-uniformities create surface tension gradients which through the stresses boundary condition lead to the so called Marangoni effect.

In the particular case of the creation of a very thin liquid film in the system a disjoining pressure term must be included in the equations [23,24]. The above described system of equations is a free boundary problem (the shape of the interface is part of the solution) and its numerical solution is extremely difficult so some assumptions are necessary to proceed with approximate solutions. Recently, numerical techniques capable of incorporating all the above phenomena have been reported but they are still applicable to simpler geometries than the present one [25].

A first assumption is that the velocities of the fluid induced by the slow external motion are relatively small compared to the pressure terms in the normal stress boundary condition. A second assumption is that the mixing induced by convection ensures that the surface concentration of a surfactant is always uniform at its equilibrium value as the gas–liquid interfaces evolve. These two assumptions permit the decomposition of the initial problem to two subproblems: The first sub-problem stands for the evolution of the shape of the liquid bridge (and internal bubble) considering a quasi-steady equilibrium shape at every instant. This shape is dictated by a static equilibrium condition and the current value of parameters such as length of liquid bridge (distance between rods), liquid volume, internal bubble size or pressure in gas line. The second sub-problem stands for the flow field in the evolving fluid domain defined by the first subproblem. In the present

Please cite this article as: Kostoglou M, Karapantsios TD, On the identification of liquid surface properties using liquid bridges, Adv Colloid Interface Sci (2014), http://dx.doi.org/10.1016/j.cis.2014.04.007

ARTICLE IN PRESS

context, only the first subproblem is of interest since the liquid flow field does not interfere with the imposed alternating electric current and the shape of the liquid bridge fully determines its electrical conductance which is the experimentally measured quantity.

The system shape can be found by minimizing the following functional expression which corresponds to the total energy of the system:

$$E = (\text{external surface energy}) + (\text{bubble's surface energy}) + (\text{potential energy induced by the gravitational field}) + (\text{thin film interaction energy}).$$

The first three terms refer to the energy of the gas–liquid interface (bridge and internal bubble) and to the gravity force. The last term is in general difficult to be quantified requiring a considerable theoretical and numerical effort due to the complicated interactions and forces that stabilize the film. An alternative approach is suggested here: The film energy term is ignored for the computation of the shape of the bridge but its significance is estimated from the deviation between the theoretical calculations and the experimental measurements for the bridge shape evolution.

2.2. The equilibrium problem

According to the above discussion only the equilibrium shape of the liquid bridge system must be resolved for the purposes of the present work. The combined liquid bridge–bubble problem will be discussed first since it includes the pure liquid bridge problem as a sub-case. A generalized approach to the equilibrium shape of the system requires the minimization of its total energy (incorporating surface and gravitational potential energies) under given sets of constraints. Typically these constraints can refer to the position of the contact lines (for pinned bubbles/bridges; so called r-type conditions) [26] or to the contact angle values (for free standing pendant/sessile bubbles/bridges; so called θ-type conditions) [27] including all possible combinations. Additional constraints are the total volume of the liquid in the bridge and of the gas in the bubble. A great simplification results from the fact that the global minimization problem can be decomposed to separate minimization subproblems for the liquid bridge and the bubble. The coupling between the two subproblems is only through curvature induced pressure jumps at the corresponding gas–liquid interfaces and through the volume conservation requirement.

Let us assume a liquid bridge between two rods of radius R and distance D between them (see Fig. 1). The surface tension is denoted as γ and the liquid-rod contact angle as θ. A cylindrical coordinate system r, X pointing upwards with X = 0 at the basis of the liquid bridge, is considered. The shape r = Y(X) of the liquid bridge is governed by the following Young–Laplace equation [28]:

$$-\frac{d^2Y}{dX^2}\left(1+\left(\frac{dY}{dX}\right)^2\right)^{-3/2}+\frac{1}{Y}\left(1+\left(\frac{dY}{dX}\right)^2\right)^{-1/2}=H-\frac{\rho g}{\gamma}X \tag{1}$$

where ρ is the liquid density and g is the gravitational acceleration. Let us assume now that a gas bubble in the liquid bridge attached at the upper rod. It is convenient to introduce a second cylindrical coordinate system r, x pointing downwards with x = 0 at the tip of the bubble. Denoting $r = Y_b(x)$ the profile of the bubble the governing equation results as [29]:

$$-\frac{d^2Y_b}{dx^2}\left(1+\left(\frac{dY_b}{dx}\right)^2\right)^{-3/2}+\frac{1}{Y_b}\left(1+\left(\frac{dY_b}{dx}\right)^2\right)^{-1/2}=F-\frac{\rho g}{\gamma}x. \tag{2}$$

The above equations are of second order so they require two boundary conditions on the edges of their definition domain. The unknown parameters H and F are determined from the fulfillment of the volume constraints. These parameters are related with the pressure in the liquid P_L and in the gas bubble P_B as: $P_{L1} - P_{atm} = \gamma H$ and $P_B - P_{L2} = \gamma F$ where P_{atm} is the external (atmospheric) pressure, P_{L1} is the pressure at the basis of the bridge and P_{L2} is the pressure at the tip of the bubble.

The second order differential Eqs. (1) and (2) must be transformed to system of first order ones. The usual approach of considering dY/dX as the second dependent variable does not perform well. It has been found that alternative variables must be used to facilitate the convergence of the problem. The best choice for the liquid bridge is the transformation to the following system:

$$\frac{d\Phi}{dX}=\frac{1}{\sin(\Phi)}\left(H-\frac{\rho g}{\gamma}X\right)-\frac{1}{Y} \tag{3}$$

$$\frac{dY}{dX}=\frac{1}{\tan(\Phi)} \tag{4}$$

where Φ is the (gas side) angle between the liquid bridge profile and the horizontal plane. The r-type boundary conditions are $Y(0) = Y(D) = R$ whereas the θ-type ones are $\Phi(0) = \pi - \theta$ and $\Phi(D) = \theta$.

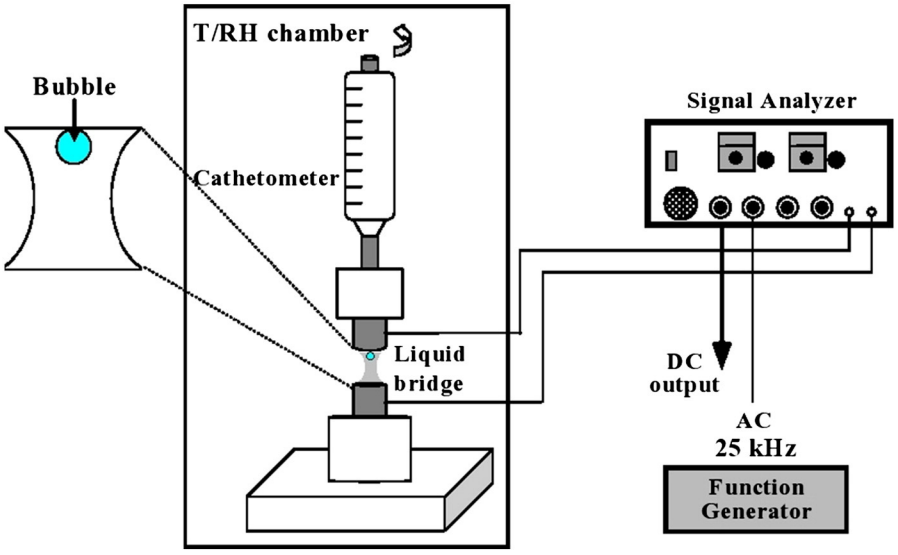

Fig. 1. Schematic diagram of the experimental setup.

Please cite this article as: Kostoglou M, Karapantsios TD, On the identification of liquid surface properties using liquid bridges, Adv Colloid Interface Sci (2014), http://dx.doi.org/10.1016/j.cis.2014.04.007

The best choice for the bubble is the following system:

$$\frac{dx}{d\psi} = \sin(\psi)\left(\frac{\sin(\psi)}{Y_b} + \frac{\rho g}{\gamma}x - F\right)^{-1} \tag{5}$$

$$\frac{dY_b}{d\psi} = -\cos(\psi)\left(\frac{\sin(\psi)}{Y_b} + \frac{\rho g}{\gamma}x - F\right)^{-1} \tag{6}$$

where the angle ψ takes values from zero at the tip of the bubble to $\pi - \theta$ at the contact line. The initial condition for the above system is $x(0) = Y_b(0) = 0$. Denoting as d the distance from the tip of the bubble to its basis the bubble gas volume constraint is given as:

$$V_b = \pi \int_{-d}^{0} Y_b^2(x)dx. \tag{7}$$

In case of θ-type conditions the integration domain is from $\psi = 0$ to $\psi = \pi - \theta$ and F can be determined from the volume constraint (7). In case of r-type conditions with contact radius R_b the integration domain and the value F must be found to simultaneously fill $Y_b = R_b$ and the volume constraint (7). In order to put the bubble to the coordinate system of the bridge the following transformation is needed: $x = (D - X) - d$. The coupling between the bridge and the bubble sub-problems is made through the pressure and through the liquid volume constraint

$$V_L = \pi \int_{0}^{D} \left(Y^2 - Y_b^2\right)dX. \tag{8}$$

The closure in the pressure relation is achieved by employing the relation $P_{L1} - P_{L2} = (D - d)\rho g$. Setting specific boundary conditions (r-type and θ-type) and specific requirements for the total liquid and bubble gas volume, the above systems of equations can be separately integrated for the shapes of the bridge and the bubble and the pressure in the liquid and in the gas. The non-linearity of the equations induces a high sensitivity with respect to their boundary conditions rendering very difficult the choice of initial guesses for problem parameters that lead to convergence. This is typically overcome using some kind of continuation process i.e. starting from a problem with known solution (e.g. a cylindrical liquid bridge and a spherical bubble) and following a specific pathway until to reach the required conditions. In the present case it is imperative to follow a computational pathway that coincides to the experimental pathway in order to vastly accelerate the solution procedure.

Let us assume that a bubble is produced internally in the liquid bridge and then the main experiment starts by increasing the distance between the rods. In this case it is not exact to set that the bubble volume is fixed through bridge lengthening. A more physical constraint is that the total mass of the gas in the bubble and in the gas chamber remains constant. This is not equivalent to the constant volume constraint since the pressure in the bubble changes as the length of the bridge evolves so the product pressure × volume (proportional to mass of the gas) must remain constant. Obviously, the coupling between the bridge and the bubble problems is complex in this case, but still it remains one-point coupling. The picture is complete now only for an insoluble in the liquid gas. Additional complications arise for soluble gases. In this case the solubility varies with the pressure in the bubble through the Henry law and (if the time is enough) the gas is absorbed in the liquid so the constant mass constraint is no more valid.

The above discussion revealed the complexities arising when a particular experimental pathway of the system needs to be modeled. Until now the modeling of the system has been restricted to constant bubble size assumption. Nevertheless, the relaxation of this assumption is required to improve the theoretical understanding of the problem on one hand and the exploitation of the experimental data on the other. The complete construction of the experimental pathway is based on the integration of the bridge equations taking into account the bubble existence and the integration of the bubble equations taking into account the pressure in the liquid. The basic aspect of the continuation/boundary value problem integration procedure will be described here for the case of the lengthening of a single r-type liquid bridge.

The boundary value problem for the liquid bridge is usually solved indirectly i.e. assuming values for H and for $\Phi(0)$ and integrating the resulting initial value problem e.g. [30]. The distance between the rods is given from $Y(D) = R$ and the liquid volume from Eq. (8). A semidirect approach that can be found in the literature (e.g. [31,32]) is to assume a value for one of H or $\Phi(0)$ and to find the other in order for V or D to take a required value. Having a scope to follow experimental pathways, it is preferable to use a direct approach for the solution of the boundary value problem (e.g. [33]). A simple shooting method is the most effective numerical technique choice. First, a value of H and $\Phi(0)$ is assumed and the initial value problem is integrated with the use of an explicit Runge Kutta integrator with self-adjusted step and prespecified accuracy [34] to find Y(D) and V values (prime stand for temporal value). The Newton Raphson method with numerically computed derivatives is used for the correction of the H and $\Phi(0)$ values. The convergence has been achieved when $Y(D) = R$ and $V = V$ (required volume value). So, in principle, for every pair of D and V values the liquid bridge shape can be computed from the above procedure. According to the continuation procedure, as the experimental pathway is followed, (D or V evolution) the initial guesses of H and $\Phi(0)$ are taken equal to the converged values of the previous step on the path. The procedure in case of presence of a constant volume bubble is exactly the same but accounting for the bubble in the volume constraint. A similar procedure can be used for the integration of the bubble shape problem.

2.3. Electrical conductance computation

Given that the frequency of the employed alternating current is such that only a resistance and not a capacitance effect is present, the alternating current can be handled as a continuous one. The potential distribution in the liquid bridge in case of an electrical potential difference between the rods is given by the solution of the following Laplace equation

$$\frac{1}{r}\frac{\theta}{\theta r}r\frac{\theta P}{\theta r} + \frac{\theta^2 P}{\theta X^2} = 0 \quad \text{in } Y_b(X) < r < Y(X) \text{ and } 0 < X < D \tag{9}$$

where P is the electrical potential normalized to be 1 at the one rod and 0 at the other.

The boundary conditions for the above equation are

$$P = 1 \text{ for } X = 0 \text{ and } 0 < r < 1 \tag{10a}$$

$$P = 0 \text{ for } X = D \text{ and } 0 < r < 1 \tag{10b}$$

$$\left(\frac{\partial P}{\partial \vec{n}}\right)_{r=Y(X)\,\cup\, Y_b(X)} = 0 \tag{10c}$$

where $\vec{n}$ is the unit normal vector. Having found the potential distribution in the bridge, the dimensionless conductance K_{app} can be computed from the relation

$$K_{app} = -\frac{2}{R}\int_{0}^{R}\left(\frac{\partial P}{\partial X}\right)_{X=0} rdr. \tag{11}$$

Please cite this article as: Kostoglou M, Karapantsios TD, On the identification of liquid surface properties using liquid bridges, Adv Colloid Interface Sci (2014), http://dx.doi.org/10.1016/j.cis.2014.04.007

ARTICLE IN PRESS

The apparent conductance is the actual conductance normalized with respect to πσR where σ is the specific electrical conductivity of the liquid and R is the radius of the basis of the bridge. The mathematical problem (9–11) is quite similar to the extensively studied problem of heat transfer in fins [35]. It can be solved using typical numerical discretization methods. A second order finite different discretization using a rectangular grid has been proposed (in the absence of bubble) in [36]. The resulting system of equations is solved using the iterative Gauss–Seidel method. Finite element computation has been performed in the presence of bubble in [37] using a specialized code. Presentation of the isopotential lines reveals the small deviation of the electric field from uni-directionality. The requirement of fitting the experimental data may require computation of conductance for hundreds of geometric configurations of the system as the experimental pathway is followed (e.g. as distance between rods or liquid volume varies). This is why an approximate simplified way to compute K_{app}, instead of solving a partial differential equation, is very useful. The almost uni-directionality of the electrical field in the bridge allowed a perturbation expansion of the conductance problem with respect to the slope of the gas–liquid interface shape [38]. The more uniform the liquid cross-section area in the X direction the more close the problem to one-dimensionality. The resulting perturbation problem is a singular one and after an extensive analysis leads to (in the absence of bubble):

$$K_{app} = I_1^{-1}\left(1-\frac{I_2}{2I_1}\right) \tag{12}$$

where

$$I_1 = \int_0^D \frac{R}{Y^2(X)}dX \tag{13}$$

$$I_2 = \int_0^D \frac{R}{Y^2(X)}\left(\frac{dY}{dX}\right)^2 dX. \tag{14}$$

The integral I_1 is the first order expansion term and it is known from the corresponding heat transfer problem. The second term becomes important as the bridge is deformed significantly especially prior to rupture. A straightforward extension of the first term to the case of the existence of bubble leads to

$$K_{app} = \left(R\int_0^D \left[Y^2(X)-Y_b^2(X)\right]^{-1}dX\right)^{-1}. \tag{15}$$

Comparison of the approximate solution with numerical results showed that whereas the second order expansion is needed in no bubble case (especially close to the rupture point) the first order expansion is enough in case of bubble existence. This is not surprising considering that the bubble prevents the deformation of the external surface of the bridge.

3. Experimental set-up

The different variations of the experimental setup have been described in detail in [36–39]. The basic experimental configuration is shown in Fig. 2. A small liquid bridge is formed between the tips of two equal solid rods, aligned vertically inside a temperature/humidity regulated chamber. The upper rod is coupled with a precision cathetometer with a resolution of 5 μm/division. The cathetometer is used to adjust the separation distance between the rods (the lower rod is permanently fixed). Rods are constructed of either stainless steel or copper which are both excellent electrical conductors. The free edges of the rods are carefully machined to be knife-edged circles in order to pin stably the three-phase contact line of r-bridges. Rods of varying radius from 0.8 to 8 mm, depending on the type of the experiments, are constructed.

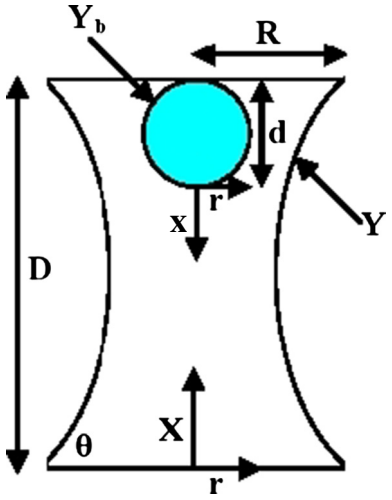

Fig. 2. Schematic of the liquid bridge–bubble system and coordinate system definition.

The liquid used is either filtered deaerated tap water (~700 μS/cm at 25 °C) or deionized water (~5 μS/cm at 25 °C) where a small amount of NaCl has been added to yield the ionic strength of deaerated tap water. This small concentration of salt does not affect interfacial properties. It must be stressed that the present electrical technique is fully functional down to liquid's electrical conductivity of around 10 μS/cm. The surface tension of the test liquid determined by both the Wilhelmy slide and the ring method measures 64–68 ± 0.2 mN/m. For thin film experiments, tests are conducted using sodium dodecyl sulfate (SDS) solutions in deionized water at concentrations below the CMC value (2400 ppm). An ultra-precision microsyringe is used to deposit the fluid that forms the liquid bridges with an error in liquid volume determination of 1% at most.

3.1. Type of experiments

(i) Increasing length of bridges at constant volume
Experiments are conducted with small bridge volumes (less than 5 μl) selected such as to not only produce a satisfactory span of electrical responses but also diminish gravity effects. Each experiment starts with setting the separation distance between the rods and forming a liquid bridge of precisely known volume with approximately cylindrical shape. The precise initial shape of the liquid bridge is not a matter of concern since the data reduction analysis takes care of it. In runs with r-bridges the bridge remains attached to the solid rods at their circular edge. In runs with θ-liquid bridges the liquid wets the solid surface at the center of the rods far away from the circular edges. The separation of the bridge is increased slowly, first in linear steps of 250, 150 or 100 μm, this being followed by gradually smaller steps down to 5 μm at the vicinity of bridge rupture. At each separation distance between the supporting rods, a high resolution picture of the bridge is taken.
During the meniscus displacement, the apparent electrical conductance of the bridge is recorded. The conductance probe comprises of the two metallic rods serving as electrodes. An a.c. carrier voltage ranging between 1.5 and 0.5 V (peak-to-peak) is applied across the probe at a frequency of 25 kHz in order to suppress undesirable electrode polarization and capacitive impedance. The response of the probe is fed to a special analyzer-demodulator. The analog d.c. voltage output of the analyzer is

Please cite this article as: Kostoglou M, Karapantsios TD, On the identification of liquid surface properties using liquid bridges, Adv Colloid Interface Sci (2014), http://dx.doi.org/10.1016/j.cis.2014.04.007

converted to equivalent conductance K_{app} of the liquid between the electrodes using a calibration curve based on precision resistors. The acquired apparent conductance values are normalized with respect to values for the initially deposited liquid bridges in order to eliminate errors in liquid conductivity measurements. At least five records are acquired at all experimental conditions and the reproducibility is good. Pearson correlation coefficients among sampled curves are always above 0.98 whereas average instantaneous signal deviations are around 3%.

(ii) Decreasing volume of bridges at constant length
Each experiment starts with initially setting the separation distance between the rods. Then, a liquid bridge of precisely known volume is formed. The liquid volume is selected such that it allows sufficient time for evaporation to snap the bridge. The initial shape of the liquid bridge is not a matter of concern since the data reduction analysis takes care of it. In all experiments the liquid bridge is considered to remain attached to the solid rods at their circular edge.
During the meniscus displacement – as a result of liquid evaporation – the apparent electrical conductance of the bridge is continuously recorded. Electrical features are the same as in (i). Data are acquired with a variable sampling frequency in the range 1–3 Hz. At least three records are acquired at all experimental conditions and the reproducibility was excellent. Pearson correlation coefficients among sampled curves are always above 0.99 whereas average instantaneous signal deviations are around 1%, a value close to the measured signal's noise.

(iii) Decreasing volume of bridges at constant length in the presence of an internal bubble. Thin film formation.
Bridges of 20 μl pinned to the edge of the supporting rods are produced. An ultra precision microsyringe driven slowly by a syringe pump is used to generate a small bubble inside the liquid bridge through a small hole ($r = 0.15$ mm) at the center of the upper rod. The rim of this hole is the contact line of the bubble with the upper rod during all times. Each experiment starts with forming a liquid bridge and a stable bubble inside the bridge. Then, using a syringe pump liquid is drained off the bridge through a small hole at the center of the lower rod. Drainage occurs at a constant rate up to the moment of rupture of the bridge. Experiments are conducted using four nominal drainage rates: 20, 50, 100 and 200 μl/h. A video camera is used to record at 25 fps the evolving shape of the liquid bridge during drainage. During drainage the instantaneous apparent electrical conductance of the bridge is continuously recorded in a microcomputer. Electrical features are the same as in (ii). At least three records are taken at all experimental conditions with good reproducibility. Pearson correlation coefficients among sampled curves are always above 0.97, whereas average instantaneous signal deviations are around 2%.

4. Results and discussion

In this section the main results of the up to now research on the exploitation of liquid bridges for the identification of liquid surface properties are presented and discussed. The subject is not mature and research is still needed but as it will be shown there is a potential for the development of reliable identification techniques.

It is quite surprising that despite the extensive experimental and theoretical research on liquid bridges since 1960 they have never been officially proposed as an alternative to pendant drops for the estimation of liquids' surface tension. This has been done in 2000 in an indirect way [39], seeking for a liquid mass configuration that allows the use of the electrical conductance technique. It is advantageous to present the analysis of the liquid bridge using dimensionless variables so in what follows the liquid bridge length D is normalized by R and the liquid bridge volume is normalized by πR^3. Dimensional variables will appear with their units from now on to be distinguished from dimensionless ones. The dimensionless parameter which appears is the so-called Bond number (Bo) which is defined as $Bo = \rho g R^2 / \gamma$. This number, in principle, denotes the ratio of the gravitational to surface tension forces and it determines the shape of the liquid bridge. It is worth noticing that taking Bo as a measure of the gravitational distortion of the bridge is rather misleading since Bo does not include the bridge length D. In practice, the product BoD can be regarded as responsible for bridge loss of symmetry induced by gravity.

In general the shape of r-bridges is fully determined by the dimensionless parameters D, V, and Bo. From the experimental point of view there are two ways of creating a trajectory in the phase space of the bridge shapes. The first is the stretching of the liquid bridge (increasing D while keeping constant V). The second way is the volume reduction either by allowing evaporation or by withdrawing liquid (decreasing V while keeping constant D). The first way has been examined theoretically and experimentally in [39]. The liquid bridge stretching leads to its rupture at a distance D_{rup} which depends on the liquid volume V and on the Bo number. The dependence of D_{rup} on V and Bo is shown in Fig. 3. The dependence on Bo is of particular interest since it includes the surface tension that must be determined. The sensitivity of D_{rup} on Bo depends on the V value. It starts from zero (for $V < 0.5$) and increases with V. The maximum sensitivity in the figure appears for $V = 2.5$ and $Bo < 0.5$ implying that only at this region of parameters a procedure of estimation of the Bo number (i.e. of surface tension) from conductance measurements is meaningful.

A better idea is not to use the single snapshot of the bridge rupture configuration but to follow the whole trajectory of the liquid bridge configurations as D increases. The sensitivity of the corresponding conductance curve with respect to Bo number is depicted in Fig. 4. It is better to use the ratio K_{app}/K_{cyl} to eliminate the possibility of error due to inaccuracy in the specific conductivity measurement. By K_{cyl} we denote the conductance of the bridge with V and D corresponding to cylindrical shape (nevertheless, the actual shape of this bridge is not cylindrical due to gravitational distortion) used as initial condition for the experiments. It is evident from Fig. 4 that the conductance curve shows satisfactory sensitivity with respect to Bo number at least for elongated bridges. So under certain circumstances fitting of an experimental conductance curve by the theoretical one can lead to a reliable estimation of Bo number and thus, of liquid surface tension. The fact that the whole curve must be fitted instead of a single value allows

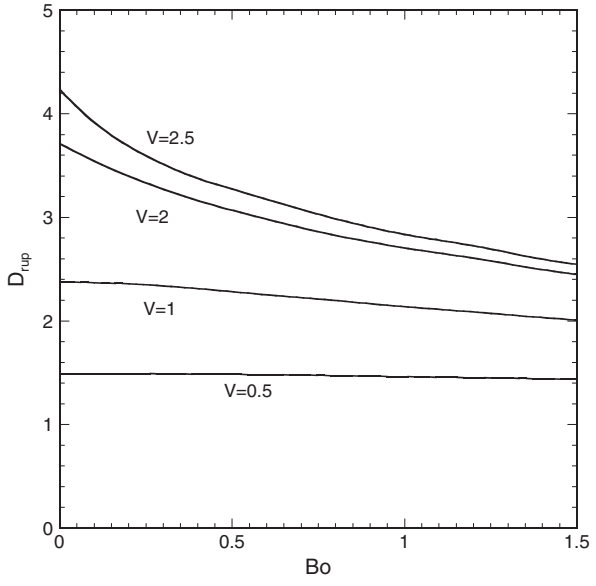

Fig. 3. Dimensionless rupture length D_{rup} versus Bond number for several values of the dimensionless volume V for an r-liquid bridge.

Please cite this article as: Kostoglou M, Karapantsios TD, On the identification of liquid surface properties using liquid bridges, Adv Colloid Interface Sci (2014), http://dx.doi.org/10.1016/j.cis.2014.04.007

ARTICLE IN PRESS

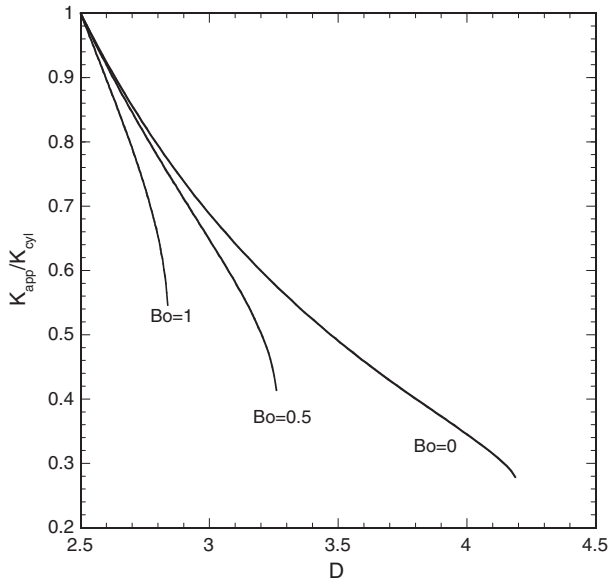

Fig. 4. Normalized apparent conductance K_{app}/K_{cyl} versus dimensionless bridge length D for dimensionless r-bridge volume V = 2.5 and several values of Bond number.

correction to small errors in the liquid volume measurement. The implementation of the proposed parameters' estimation procedure has not been pursued in [39] but the comparison between experimental and theoretical conductance curves shown in Fig. 5 was made in order to confirm the theoretical assertions.

The idea of exploring liquid bridges to estimate liquid surface tension using images of the bridges has been exhaustively studied in [40] a few years ago. The sensitivity of the liquid bridge-based analysis is compared to that of the established pendant drop method. The phase diagram of liquid bridges in V, D plane and the stretching and suction trajectories previously proposed in [39] are presented in detail. The sensitivity analysis is based on computation of the deviation between liquid bridge shape profiles derived by changing surface tension by ±2.5%. Experimental liquid bridge shapes for hexadecane and cyclohexane are used for the parameter estimation procedure leading to surface tension values within 1% of the corresponding literature values. Such sensitivity can be achieved only for liquid bridges close to their stability limit as it has been previously shown in [39]. Regarding the comparison between the liquid bridge and the pendant drop configurations it was found that the shape of a liquid bridge close to the rupture point is more sensitive to the surface tension than a pendant drop of the same volume. The accuracy in surface tension is similar for both configurations for Bo of the order of 0.1 but it is better for a liquid bridge for Bo of the order of 0.01.

The volume reduction trajectory of the liquid bridge up to rupture has been studied in [38]. The experimental volume reduction was achieved by evaporation of the liquid bridge liquid. The evaporation rate is not known and it is not constant in time so this type of experiments cannot be used for estimation of surface tension. On the other hand for known values of the surface tension the experimental conductance curve can be used for the construction of the evolution of the evaporation rate of the bridge. Theoretical curves of the apparent conductance as a function of the dimensionless liquid bridge volume V can be found in Fig. 6 for Bo = 0 and several values of D, and in Fig. 7 for D = 2.5 and several Bo numbers. Let us denote the corresponding experimental curve as $K_{exp}(t)$ where t is the time. By enforcing the curves $K_{app}(V)$ and $K_{exp}(t)$ to coincide, the evolution curve of the liquid bridge volume V(t) can be found. The evaporation rate is simply $-dV/dt$ and is shown in dimensional form versus the liquid bridge volume in Fig. 8 (experimental conditions shown in the figure). The increase of the evaporation rate as the volume of the bridge is reduced is due to the increase of the bridge surface area and to its curvature variation that leads to acceleration of the vapor diffusion in the gas phase.

The up to now discussion refers to r-bridges having a constant base radius R (pinned contact line) as V or D varies. The situation in θ-bridges in which R is unknown and evolves in time is more difficult. The simultaneous determination of surface tension and contact angle is impossible. Nevertheless, in the limit of small values of product BoD, gravity has no influence to the liquid bridge shape and subsequently the conductance curve during stretching does not depend on surface tension. The idea is to use the conductance versus D curve to estimate the contact angle θ. The theoretical dependence of the apparent conductance to the contact angle is shown in Fig. 9 (Bo = 0). The sensitivity is exploitable only close to the rupture point and it is higher for θ < 60°. Despite that the contact angle estimation idea seems to work in principle, there are fatal practical problems. The contact angle is not constant not only in time (a problem that could be handled by a simple modification of the proposed method) but also along the contact line as found by

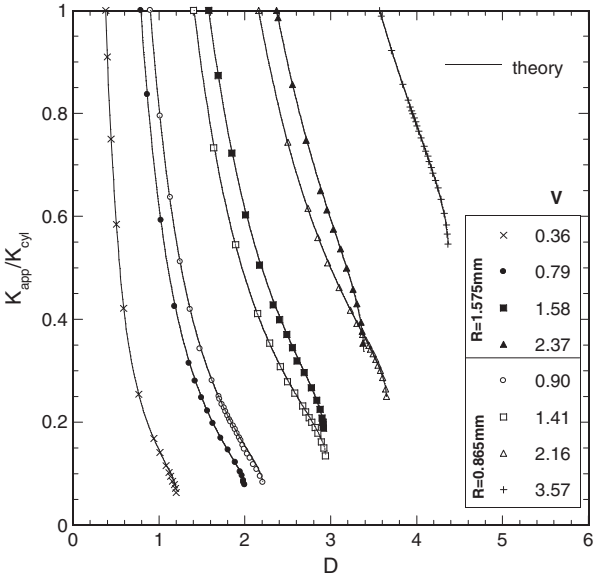

Fig. 5. Comparison between theoretical and experimental normalized apparent conductance K_{app}/K_{cyl} versus dimensionless bridge length D curves. The rod radius and the dimensionless r-bridge volume V are shown in the legend.

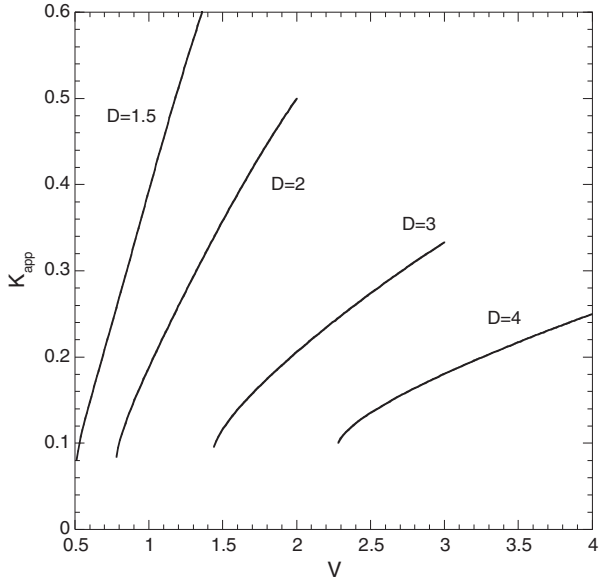

Fig. 6. Apparent conductance K_{app} versus dimensionless r-bridge volume V for zero Bond number and several dimensionless length D values.

Please cite this article as: Kostoglou M, Karapantsios TD, On the identification of liquid surface properties using liquid bridges, Adv Colloid Interface Sci (2014), http://dx.doi.org/10.1016/j.cis.2014.04.007

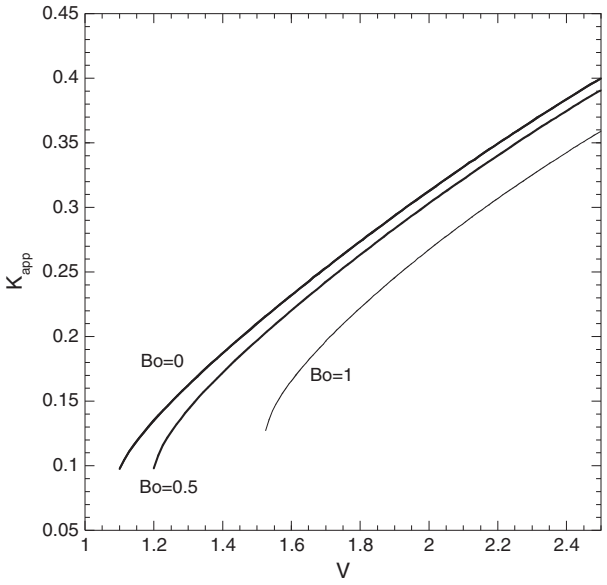

Fig. 7. Apparent conductance K_{app} versus dimensionless r-bridge volume V for dimensionless length D = 2.5 and several Bond number values.

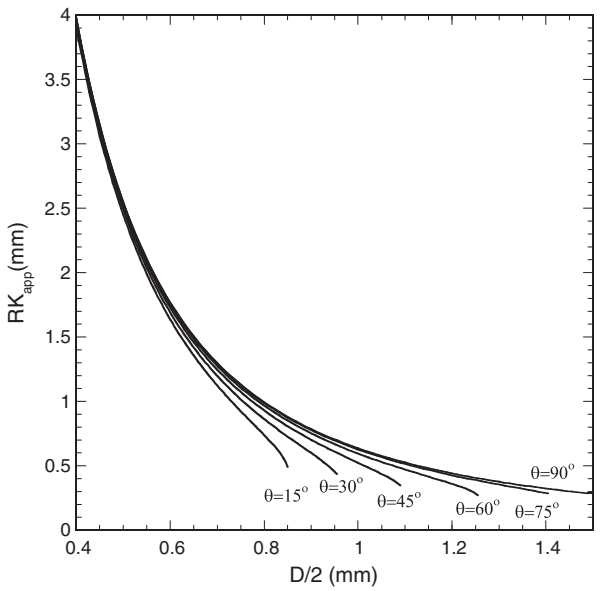

Fig. 9. Product of the θ-bridge basis radius R and apparent conductance K_{app} versus half bridge length for several values of contact angle.

optical observations [36]. The attempt to fit the experimental geometric features of the bridge by theoretical lines based on a single contact angle value leads to poor results as shown in Fig. 10 for the liquid bridge neck radius Y_e and in Fig. 11 for the base radius R. The deviation is due to the distribution of contact angle existing in practice. So the whole idea of contact angle identification through liquid bridge conductance measurement seems feasible in theory but it was proved unsuccessful in practice [36].

The previous discussion refers to pure liquids. In the presence of surfactants the situation is much more difficult. Very slow variations must be pursued experimentally to ensure equilibrium on the surface. In addition the partition of surfactant between the bulk and the evolving surface of the bridge must be taken into account by the model. The possibility of finding the static surface tension of surfactant solutions has not been explored up to now in literature.

The next idea proceeds further to the study of the dynamic surfactant effect using liquid bridge conductance measurements [37]. Additional properties as dynamic surface tension or surface elasticity can be elaborated in the presence of surfactants. In order to enhance the influence of the surfactant dynamic properties a thin film must be created and this is achieved by producing an internal bubble inside the liquid bridge. Stability experiments for bubbles internal to liquid bridges of pure liquids can be found in the literature but analysis of the results is missing [41]. Three ways have been tested for the creation of thin liquid films in liquid bridge configurations: i) creation of a bubble internally to the liquid bridge followed by liquid suction (with conductance recording) up to rupture. ii) Growth of a bubble internally to the bridge (with conductance recording) until rupture. iii) Growth of a bubble internally to a pendant drop until reaching the opposite rod and being transformed to a liquid bridge.

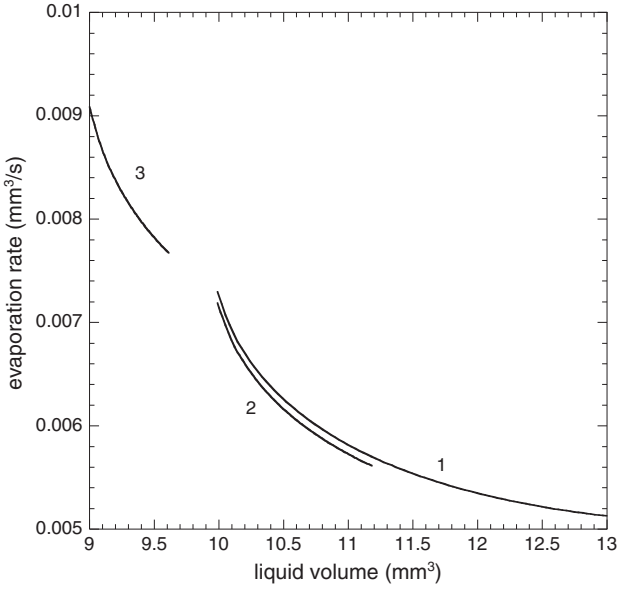

Fig. 8. Estimated evaporation rate versus current r-bridge volume for three experiments with conditions (1) R = 1.575 mm, D = 3.21 mm and V = 13.1 μl, (2) R = 1.575 mm, D = 3.21 mm, and V = 11.2 μl, and (3) R = 1.495 mm, D = 3.155 mm, and V = 9.6 μl.

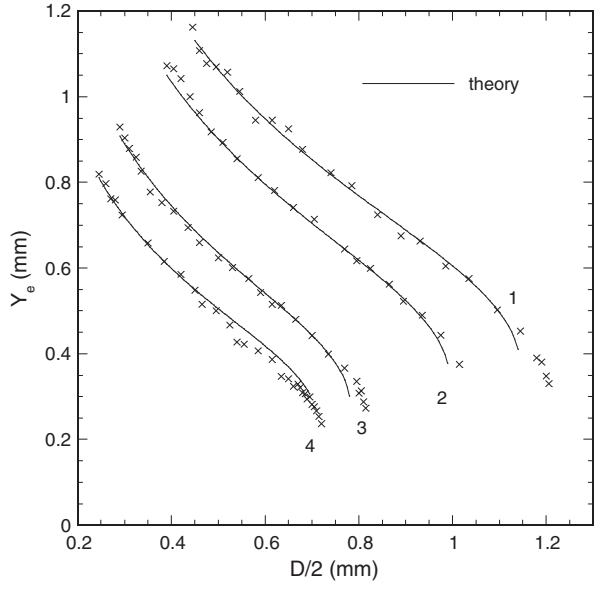

Fig. 10. Comparison between experimental and theoretical bridge neck radius Y_e versus half length of the bridge curves for four experiments. The experimental conditions are (1) V = 2 μl and θ = 55°, (2) V = 1.5 μl and θ = 45°, (3) V = 0.83 μl and θ = 40°, and (4) V = 0.55 μl and θ = 45°.

Please cite this article as: Kostoglou M, Karapantsios TD, On the identification of liquid surface properties using liquid bridges, Adv Colloid Interface Sci (2014), http://dx.doi.org/10.1016/j.cis.2014.04.007

The liquid bridge survives for a short period of time during which the conductance is recorded. The third type of experiments leads to the creation of the thinner and more uniform liquid film (soap film). The size evolution of the growing bubble is difficult to be determined experimentally for technical reasons and it is even more difficult to be modeled. On the contrary, the size evolution of the bubble during suction of the liquid can be modeled as it has been shown in the Theoretical framework section. So the experimental procedure (i) seems to be more advantageous for the study of the surfactant dynamic properties. A set of experiments for several concentrations of aqueous solutions of SDS and several suction rates has been performed. The suction rate is important in this case since dynamic phenomena are under consideration. The direct modeling of the experimental procedure to find explicitly physical parameters is not possible. The idea already discussed is to ignore in the model the thin film energy term and to attribute the difference between the theory and experiment to this term.

It is noted here that the film energy term includes not only a static contribution (e.g. disjoining pressure) but also a dynamic contribution (e.g. Gibbs–Marangoni elasticity associated to surfactants). The assumption of an equilibrium concentration of surfactant made for the largest part of the bridge surface does not hold in the region of the very thin film near the bubble's equator. Macroscopic equilibrium properties such as the Gibbs elasticity of the bridge are taken into account by the model employing the adsorption isotherm and the surface tension — concentration relation for the particular surfactant employed. Typical comparison between experimental and modeled conductance is shown in Fig. 12 (initial liquid volume: 20 μl, bubble radius: 0.6 mm, rod radius: 1.6 mm, bridge length: 3 mm). The conductance is normalized by its initial value K_o to eliminate uncertainty associated with the liquid specific conductivity value. The discrepancies appeared at intermediate times have to do with the constancy of the suction rate and they are not important in the present context. The important region here is the one before rupture where a thin film appears. The details cannot be observed in the scale of Fig. 12 so a magnification is given in Fig. 13. The effect of surfactant on the system behavior is quite obvious. The physical phenomena leading to the appearance and stabilization of the thin film are described in Fig. 14. It is noted that the film creation cannot be optically followed for technical reasons so the conductance technique is crucial for this type of experiments. The main parameter derived from the experiments is the thin film survival time (t_{rup}) as a function of the suction rate. This parameter is a measure of the surface

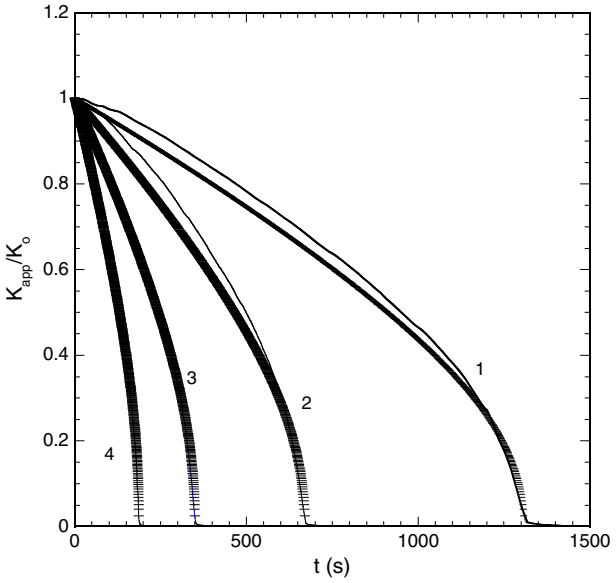

Fig. 12. Normalized apparent conductance evolution during liquid suction from a liquid bridge with a bubble inside the bridge (initial liquid volume: 20 μl, bubble radius: 0.6 mm, rod radius: 1.6 mm, bridge length: 3 mm) for 2000 ppm SDS concentration and for four values of liquid suction rate: (1) 20 μl/h, (2) 50 μl/h, (3) 100 μl/h, and (4) 200 μl/h.

elasticity induced by the surfactant. Further research is needed to relate this parameter to specific surfactant properties or directly to the performance of surfactant in practical applications (e.g. foam stability).

5. Conclusions

In the present work a review of the use of liquid bridge configuration as a tool for estimation of surface properties is presented. Despite the extensive studies on liquid bridges in the literature the liquid bridge configuration as a diagnostic tool has been very little explored in the past. Only recently it was shown that the liquid bridge shape is more sensitive to surface tension than the pendant drop shape. The distinct advantage of the liquid bridge configuration is that it allows passing of electric current (for conducting liquids). This offers the possibility to

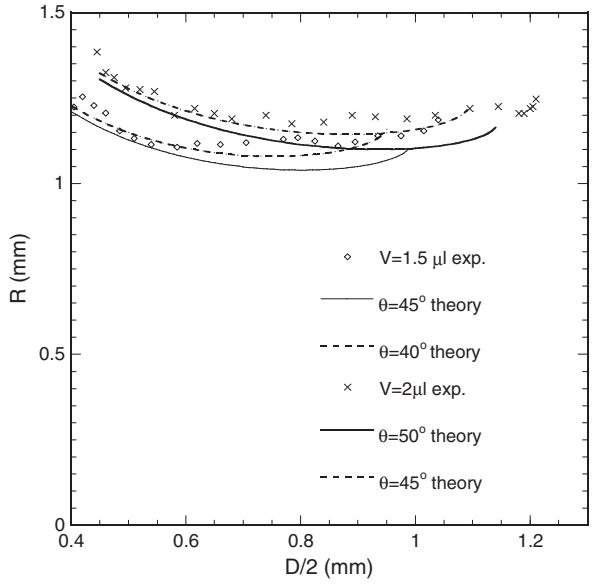

Fig. 11. Comparison between experimental and theoretical bridge base radius R versus half length of the bridge curves, for two experiments.

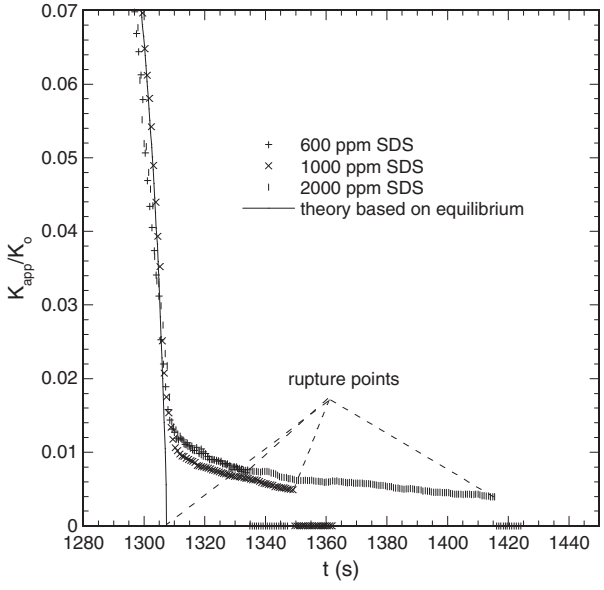

Fig. 13. Detail magnification of the normalized apparent conductance evolution curve for several SDS concentrations and for liquid suction rate of 20 μl/h.

Please cite this article as: Kostoglou M, Karapantsios TD, On the identification of liquid surface properties using liquid bridges, Adv Colloid Interface Sci (2014), http://dx.doi.org/10.1016/j.cis.2014.04.007

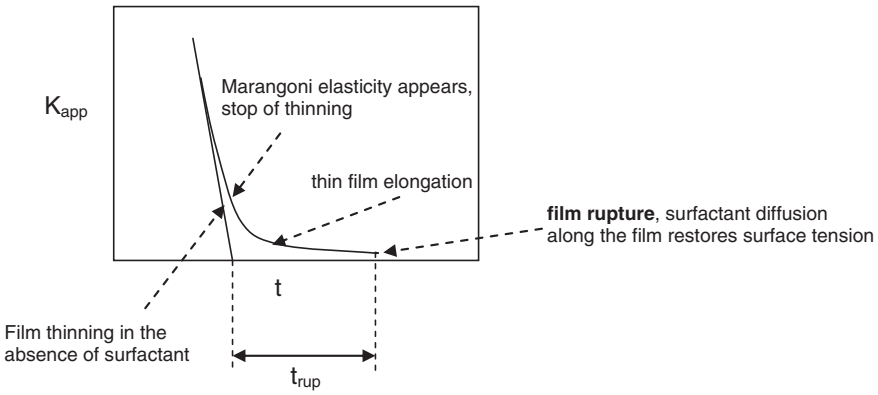

Fig. 14. A survey of phenomena occurring during water suction from the liquid bridge–bubble configuration.

measure the bridge electrical conductance as an alternative integral shape descriptor in place of the integral force measurement or the detailed optical imaging. Comparison of the theoretical and experimental conductance curves created by varying a bridge parameter (liquid volume or bridge length) can lead to estimation of some surface property. The whole approach seems to have potential for estimating the surface tension of conducting liquids. On the contrary, the attempt to estimate contact angle has been proved rather unsuccessful. The variation of the method with a bubble formed internally to the bridge exhibits good prospect as a tool for estimation of surface elasticity (thin film stabilization) induced by surfactant addition. In any case, more theoretical and experimental work is needed for further development of the above idea towards establishment of liquid bridge based surface property diagnostic techniques.

References

[1] Simons SJR, Sevile JPK, Adams MJ. Chem Eng Sci 1994;49:2331.
[2] Nguyen AV, Schulze HJ. Colloidal science of flotation. Marcel Dekker; 2004.
[3] Mort PR. Powder Technol 2005;150:86.
[4] Chadra S, Batur C. Eng Appl Comput Mech 2010;4:181.
[5] Pelesko JA. Self assembly—the science of things that put themselves together. Chapman Hall/CRC; 2002.
[6] Syms RA, Yeatman EM, Bright VM, Whitesides GM. J MEMS 2003;12:387.
[7] Forget M, O'Donnell M, Davies M. Proc Inst Mech Eng C J Mech Eng Sci 2008;222:777.
[8] Men YM, Zhang XR, Wang WC. J Chem Phys 2009;131 [Article Number: 184702].
[9] Wei Z, Zhao YP. J Phys D Appl Phys 2007;40:4368.
[10] Patel NM, Taylor PL, Fisch MR, Rosenblatt C. Colloids Surf A Physicochem Eng Asp 2003;218:65.
[11] Liao YC, Subramani HJ, Franses EI, Basaran OA. Langmuir 2004;20:9926.
[12] Deganello D, Williams AJ, Croft TN, Lubansky AS, Gethin DT, Claypole TC. Comput Fluids 2011;40:42.
[13] Herrada MA, Lopez-Herrera JM, Vega EJ, Montanero JM. Phys Fluids 2011;23 [Article Number: 012101].
[14] Kuhlmann HC. Thermocapillary convection in models of crystal growth. Springer Verlang; 1999.
[15] Bazilevsky AV, Entov VM, Rozhkov AN. Fluid Dyn 2011;46:613.
[16] Fainerman VB, Aksenenko EV, Petkov JT, Miller R. Colloids Surf A Physicochem Eng Asp 2011;385:64.
[17] Cabezas MG, Bateni A, Montanero JM, Neumann AW. Appl Surf Sci 2004;238:480.
[18] Wolfram E, Pinder J. Acta Chem Acad Sci Hung 1979;100:433.
[19] Drygiannakis AI, Papathanasiou AG, Boudouvis AG. J Colloid Interface Sci 2008;326:451.
[20] Woisetschlager J, Wexler AD, Holler G, Eisenhut M, Gatterer K, Fuchs EC. Exp Fluids 2012;52:193.
[21] Moulton DE, Pelesko JA. J Colloid Interface Sci 2008;322:252.
[22] Leal LG. Advanced transport phenomena: fluid mechanics and convective transport processes. Cambridge University Press; 2007.
[23] Dukhin SS, Kretzschmar G, Miller R. In: Mobius D, Miller R, editors. Dynamics of adsorption at liquid interfaces. , Studies in interface scienceAmsterdam: Elsevier; 1995.
[24] Starov VM. J Colloid Interface Sci 2004;269:432.
[25] Olgac U, Muradoglu M. Int J Multiphase Flow 2013;48:58.
[26] Boucher EA, Evans MJB. J Colloid Interface Sci 1980;75:409.
[27] Boucher EA, Evans MJB, McGarry SJ. J Colloid Interface Sci 1982;89:154.
[28] Zasadzinski JAN, Sweeney JB, Davis HT, Scriven LE. J Colloid Interface Sci 1987;119:108.
[29] Pozrikidis C. Fluid dynamics. Theory, computation and numerical simulation. Kluwer; 2001.
[30] Fortes MA. J Colloid Interface Sci 1982;89:154.
[31] Mazzone DN, Tardos GI, Pfeffer R. J Colloid Interface Sci 1986;113:544.
[32] Lian G, Thornton C, Adams MJ. J Colloid Interface Sci 1993;161:138.
[33] Spencer JL, Gunde R, Hartland S. Comput Chem Eng 1998;22:1129.
[34] Press WH, Teukolsky SA, Vetterling WT, Flannery BP. Numerical recipes. Cambridge University Press; 1992.
[35] Michailov MD, Özisik MN. Unified analysis and solutions of heat and mass diffusion. Wiley; 1984.
[36] Evgenidis S, Kostoglou M, Karapantsios TD. J Colloid Interface Sci 2006;302:597.
[37] Kostoglou M, Georgiou E, Karapantsios TD. Colloids Surf A Physicochem Eng Asp 2011;382:64.
[38] Karapantsios TD, Kostoglou M. J Colloid Interface Sci 2002;255:177.
[39] Kostoglou M, Karapantsios TD. J Colloid Interface Sci 2000;227:282.
[40] Ferrera C, Montanero JM, Gabezas MG. Meas Sci Technol 2007;18:3713.
[41] Dodds S, Carvalho SD, Kumar S. Langmuir 2011;27:1556.

Please cite this article as: Kostoglou M, Karapantsios TD, On the identification of liquid surface properties using liquid bridges, Adv Colloid Interface Sci (2014), http://dx.doi.org/10.1016/j.cis.2014.04.007